08

Formation of transport layers of titanium dioxide with fractal-percolation structure

© E.N. Muratova[1], A.Yu. Gagarina[1], V.P. Bezverkhniy[1,¶], V.A. Moshnikov[1], A.I. Maksimov[1], D.A. Kozodaev, I.A. Vrublevsky[2], N.V. Lushpa[2]

[1] St. Petersburg State Electrotechnical University „LETI"
St. Petersburg, Russia
[2] Belarusian State University of Informatics and Radioelectronics,
Minsk, Belarus

¶ E-mail: vlad150897@yandex.ru

Received April 30, 2025
Revised September 8, 2025
Accepted November 11, 2025

A method for forming a nanostructured titanium dioxide layer by oxidation of a two-layer Al|Ti coating by electrochemical anodizing is proposed and implemented. A special feature of the layer is the preservation of conductive (percolation) properties during fractalization of the structure. The synergistic effect of the combination of the fractal structure of the transport layer, which prevents the degradation of the working layer of the solar cell, and the appearance of percolation conducting channels at the interface of the resulting oxide phases of titanium and aluminum, is promising for the development of interlayer design. Atomic force microscopy techniques have been applied to analyze the nanoarchitectonics of the layers.

Keywords: nanoarchitectonics, electrochemical oxidation, Al−Ti, interface, atomic force microscopy.

DOI: 10.61011/PSS.2025.12.63104.8062k-25

1. Introduction

Nanostructured materials represent a wide class of materials used in various fields of science and technology [1]. This is attributable to the fact that layers with nanoscale structural features have properties different from bulk materials.

One of the most promising nanostructured semiconductor materials is titanium dioxide (TiO_2). Thus, t is assumed in Ref. [2] that when applying a layer of TiO_2 by the method of atomic layer deposition on a Si substrate, a titanium dioxide film is a source of oxygen for silicon oxidation. This is explained by the fact that titanium oxide is an n-type semiconductor due to excessive intrinsic defects in the oxygen sublattice of oxygen donor vacancies.

Recently, the use of TiO_2 films as a transport layer in solar cells has been considered. Thus, it was shown in Refs. [3,4] that two-layer oxidized titanium structures on aluminum can be used as *n*-transport layers in perovskite solar cells. Studies have shown that local conductivity occurs in such films due to the redistribution of charge carriers at the interface between the two oxides. At the same time, the conductivity increases by several orders of magnitude due to percolation effects [5,6].

The aim of this work was to create an effective technology that ensures fractal nanogrindity of mixed particles from the initial layers of aluminum and titanium. In this case, oxide layers will form on the Al−Ti interface. And as a result of the different electron affinity, similar to the effect found in Ref. [5], highly conductive percolation channels necessary for the transport layer will arise. In addition, nanostructuring is an effective way to reduce degradation due to ion diffusion [7,8].

The authors propose using atomic force microscopy (AFM) methods as methods of effective control of these properties — in particular, methods such as the current spreading method and topology measurements, followed by analysis of the fractal Hausdorff−Bezikovich dimension structured coatings.

2. Production of films

Al films with a thickness of 100 nm and Ti films with a thickness of 50−60 nm were deposited on silicon substrates by magnetron sputtering in argon medium at the Atis 500 installation (Izovac, Belarus). The following modes were used for applying aluminum films: source power 1.5 kW, discharge voltage — 380 V, discharge current — 3.7 A, argon pressure — $6 \cdot 10^{-2}$ Pa, residual pressure in camera — 10^{-3} Pa, film application rate — $2.8\,\mathrm{nm} \cdot \mathrm{s}^{-1}$. Ti films were applied in the following modes: source power 1.0 kW, discharge voltage 310 V, discharge current 3.0 A, argon pressure $2 \cdot 10^{-2}$ Pa, residual pressure in the chamber 10^{-3} Pa, deposition rate films $0.1\,\mathrm{nm} \cdot \mathrm{s}^{-1}$, substrate temperature at room temperature, distance between target and substrate 11 cm.

Electrochemical oxidation of Ti films was carried out in an electrolyte based on a mixture of 2% aqueous solution of oxalic acid and 1% aqueous solution of sulfamic acid (by weight). A two-electrode anodizing cell with

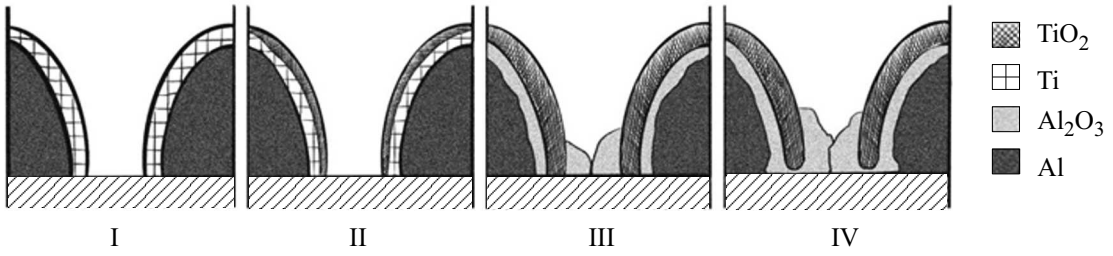

Figure 1. The scheme of formation of the oxide layer TiO_2 during electrochemical oxidation.

a titanium anode was used (sample with film Ti) and a graphite cathode. Electrochemical oxidation of Ti was carried out in the electrolyte at voltages in the range 5–50 V and subsequent exposure until the anodizing current drops to 10% of the initial level. After that, the samples were annealed at a temperature of 140°C.

3. Study of surface morphology

Anodic oxide films are formed on metals during anodic polarization in electrolyte solutions and are similar in many physical properties to oxide films formed during thermal oxidation, but at the same time differ in structure. As a result of anodizing, a two-layer oxide film is formed on the metal, in which the inner layer adjacent to the metal consists of a stoichiometric oxide, and the outer oxide layer bordering the electrolyte contains acid anion residues used in anodizing. A schematic representation of the formation of the anodized structure is shown in Figure 1.

The first stage in Figure 1 corresponds to Ti films deposited on Al. At the second stage, titanium is oxidized as a result of electrochemical etching, forming a titanium oxide film. At the third stage, after the oxidation of all titanium, aluminum begins to oxidize. Aluminum oxide has a lower density, so its formation leads to overgrowth of pores. Finally, at the fourth stage, as a result of prolonged electrochemical etching, significant overgrowth of the pores can be observed.

The obtained layers were investigated by the AFM method in semi-contact mode (probe NSG01) at the NTEGRA PRIMA installation (LLC „NOVA SPB“). Figure 2 shows AFM images of the topography of the layer of TiO_2 films obtained at different anodizing voltages.

Analysis of the topographies of the samples showed that the porosity of the titanium oxide layer is a consequence of the porosity of the initial layer of metallic titanium. The heterogeneity of the topography of the anodized samples decreases with increasing stress due to an increase in the volume of the layer materials during oxidation.

For the obtained topographies in the NovaSMM 4.0 program, height distribution statistics were constructed, shown in Figure 3.

As the voltage increases to 20 V, the pore depth, which we determined from the maximum height distribution, increases. A further increase in the anodizing voltage, on the contrary, reduces the pore depth. At the same time, the higher the voltage, the lower the depth.

Fractal dimensions D_0 of the obtained films of TiO_2

U_{anode}, V	D_0 (cubes)	D_0 (triangulation)
10	2.473	2.585
20	2.507	2.602
30	2.465	2.548
40	2.472	2.568
50	2.420	2.542

For AFM images of the morphology of the studied films, the fractal dimension D_0 was estimated using the cube method and triangulation method in the Gwyddion 2.62 [9] program (the size of AFM images $5\times5\,\mu$m). The calculation results are presented in the following table.

The fractal dimension, close to 2.5, indicates a developed surface of a porous structure close to the Brownian surface. The fractal dimension of the samples almost does not change at different anodizing stresses, which indicates the preservation of the overall morphological structure. Nevertheless, small changes in the fractal dimension with a change in the anodizing voltage have common trends when calculated using both methods. Thus, a decrease in the fractal dimension is largely associated with the overgrowth of pores. Thus, this method allows for technological control of the anodizing process.

4. Study of electrophysical properties

The formation of a fractal surface is accompanied by a change in electrophysical properties. An informative method for confirming these patterns is the method of scanning microscopy of current spreading. Figure 4 presents maps of spreading resistance, confirming the validity of the proposed model. The measurements were carried out at a negative bias voltage (−7 V). Voltage was applied to the sample, and the probe was grounded. No current was recorded with a positive bias. In the current recording system, a zero offset was recorded at the level of 1.5–1.25 nA.

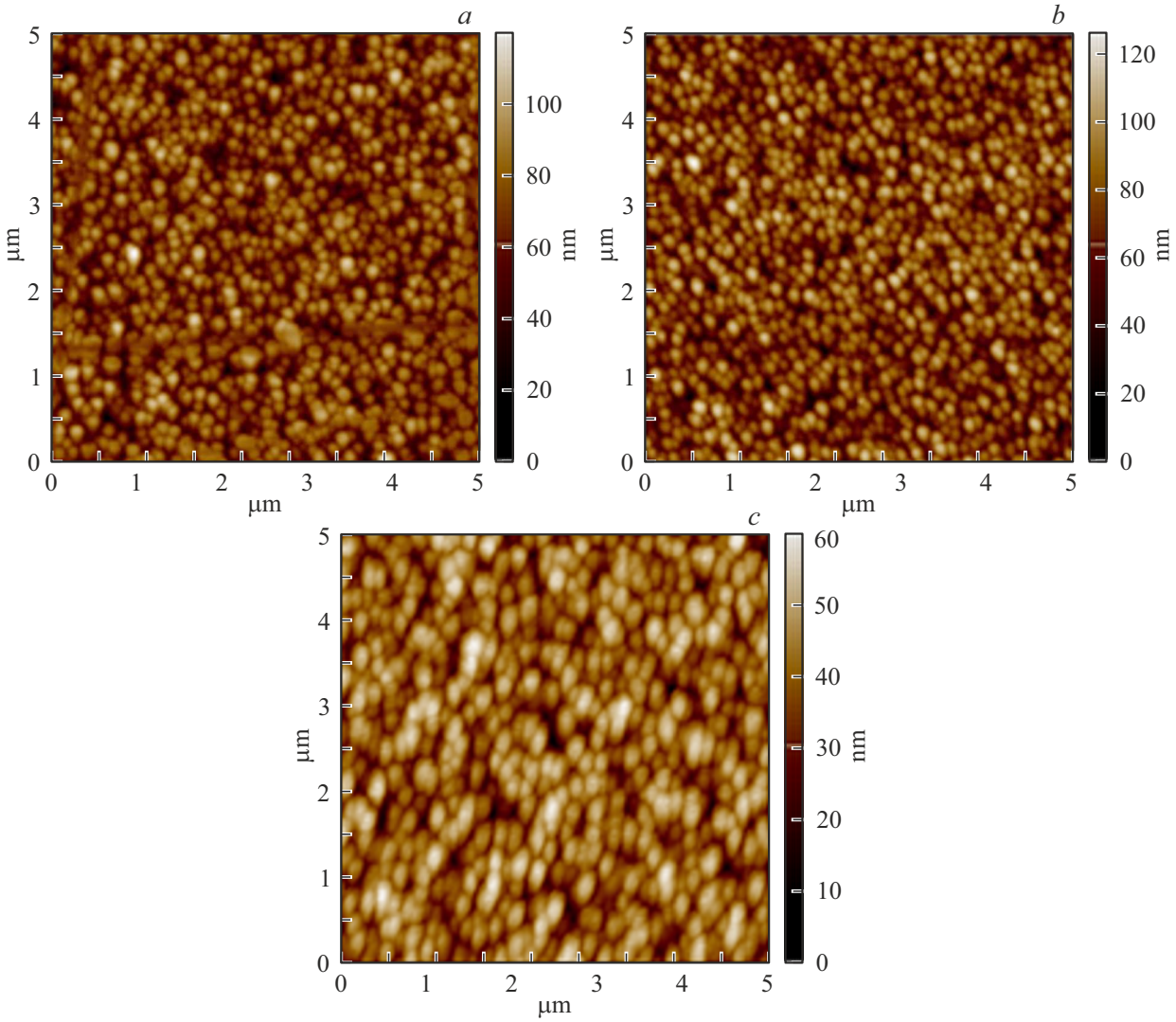

Figure 2. AFM images of TiO_2 layers at different anodizing currents: *a*) 10 V, *b*) 20 V, *c*) 50 V.

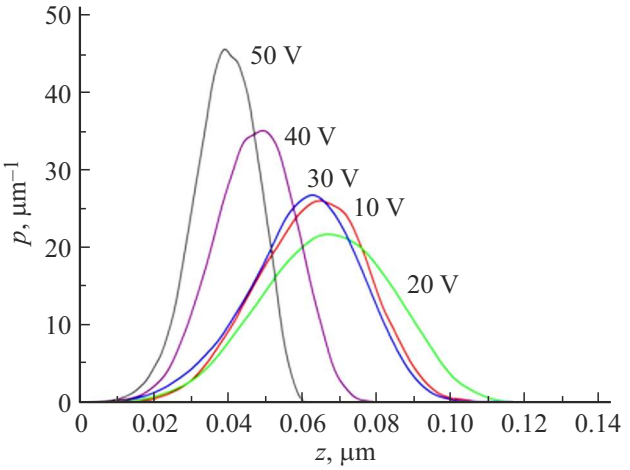

Figure 3. p is the ratio of the number of points at height z to the value of this height, for TiO_2 films obtained at different anodizing voltages.

The applied AFM techniques allow us to conclude that during anodizing up to 30 V, only titanium is oxidized to form a film of TiO_2. Titanium oxide has a lower density and grows upward, which increases the pore depth (Figure 3, Figure 1, II). At high voltages, aluminum begins to oxidize to Al_2O_3. First of all, oxidation of Al occurs between titanium grains (i. e., at the contact points of aluminum with the electrolyte), which leads to pore overgrowth, since Al_2O_3 has a lower density than Al. It should be noted that aluminum begins to oxidize after complete oxidation of titanium under the TiO_2 film (Figure 2, Figure 1, III and IV).

The second process, which affects the electrophysical properties of the oxide layers, begins with the heat treatment of the resulting two-layer structures and, therefore, proceeds independently of the anodizing process. At the same time, part of the aluminum in contact with titanium oxide begins to take on oxygen, forming vacancies in the titanium oxide layer, and restoring pure titanium from its oxide.:

$$3TiO_2 + 4Al \rightarrow 3Ti + 2Al_2O_3.$$

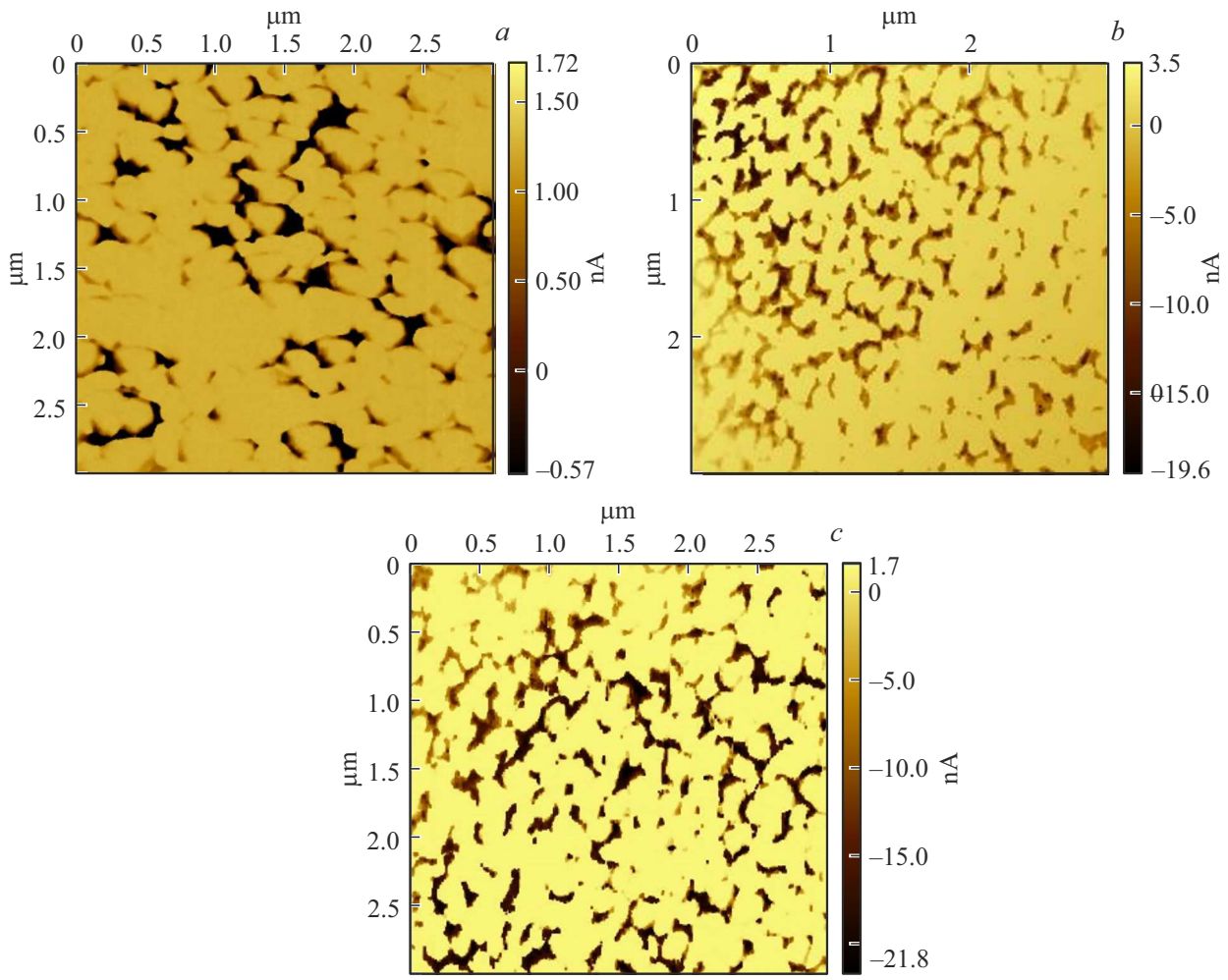

Figure 4. Microscopy maps of spreading resistance for films produced at various anodizing voltages: *a*) 10 V, *b*) 20 V, *c*) 50 V.

The result of this process is clearly visible on AFM microscopy images of the spreading currents in the depth of the pores and between the grains, because there the contact of TiO_2 and Al reaches the surface of the sample. As a result, conducting regions are observed in the pores between the grains, as shown in Figure 4, associated with changes in the conductivity of the surface and interfaces in TiO_2 grains. The resistance of the emerging conductive regions does not depend on the anodizing voltage during etching, which means that the described process took place for all samples. The mechanism proposed here is important for understanding the nature of the appearance of donor centers in anodic titanium oxide. The data shown in Figure 4 show high resistance on the grains of the formed films, and the current in these films flows through the grain interface.

5. Conclusion

It has been shown that electrochemical treatment of pre-deposited nanoscale layers of aluminum and titanium leads to the formation of a fractal nanograin structure that retains high conductivity due to the interface effect of $Al_2O_3-TiO_2$. This provides increased resistance to degradation processes due to nanostructuring. The developed methods of atomic force microscopy based on current spreading ensured the establishment of patterns of percolation current flow along grain boundaries.

Funding

The work was supported by a grant from the Russian Science Foundation No. 23-42-10029 (https://rscf.ru/project/23-42-10029).

Conflict of interest

The authors declare no conflict of interest.

References

[1] S. Ben Slama, F. Saadallah, T. Fiorido, M. Grich, F. Krout, M. Bendahan, W. Dimassi, M. Bouaicha. Silicon **16**, *15*, 5637 (2024). https://doi.org//10.1007/s12633-024-03100-x

[2] R. Methaapanon, S.F. Bent. J. Phys. Chem. C 2010, **114**, *23*, 10498 (2010). https://doi.org//10.1021/jp1013303
[3] V. Moshnikov, E. Muratova, A. Aleshin, A. Maksimov, G. Nenashev, I. Vrublevsky, N. Lushpa, A. Tuchkovsky, A. Zhilenkov, O. Kichigina. Crystals **14**, *4*, 376 (2024). https://doi.org//10.3390/cryst14040376
[4] A.Yu. Gagarina, V.P. Bezverkhny, E.N. Muratova, V.A. Moshnikov, I.A. Vrublevsky, A.K. Tuchkovsky, N.V. Lushpa. FTP **58**, *11*, 591 (2024) (in Russian). DOI: 10.61011/FTP.2024.11.59480.6580A
[5] A.A. Ryabko, D.S. Mazing, A.A. Bobkov, A.I. Maximov, V.S. Levitskii, E.F. Lazneva, A.S. Komolov, V.A. Moshnikov, E.I. Terukov. Phys. Solid State **64**, *11*, 1657 (2022).
[6] D.A. Kozodaev, A.A. Yakovleva, A.A. Bobkov, A.A. Ryabkov, V.A. Moshnikov, O.A. Korepanov. Patent for invention RU 2825297C1, 08/23/2024. Application No. 2023129274 dated 13.11.2023
[7] Z. Huang, L. Feng, X. Xia, J. Zhao, P. Qi, Y. Wang, J. Zhou, L. Shen, S. Zhang, X. Zhang. Nanoscale **16**, 2078 (2024). https://doi.org//10.1039/D3NR05461F
[8] B. Ng, X. Peng, E. Faegh, W.E. Mustain. J. Mater. Chem. A **8**, *5*, 2712 (2020). https://doi.org//10.1039/C9TA11708C
[9] https://gwyddion.net/documentation/user-guide-ru/fractal-analysis.html. Date of access 23.06.2025.

Translated by A.Akhtyamov